Drug Development and Industrial Pharmacy, 33:1240–1253, 2007

ISSN: 0363-9045 print / 1520-5762 online
DOI: 10.1080/03639040701378035

informa
healthcare

Determination of the Surface Energy Distributions of Different Processed Lactose

Frank Thielmann
Surface Measurement Systems UK, London, UK

Daniel J. Burnett
Surface Measurement Systems NA, Allentown, PA, USA

Jerry Y. Y. Heng
Department of Chemical Engineering, Imperial College London, South Kensington Campus, London, UK

Particulate interactions between drug and lactose carrier in dry powder inhaler formulations are affected by the heterogenous energy distribution on the surface of the individual compounds. A new method based on Inverse Gas Chromatography at finite concentration is applied to study the energy heterogeneity of untreated, milled, and recrystallized lactose of similar particle size distribution. Energy distributions for the dispersive surface energy and the specific free energy of ethanol are obtained. Milling causes an increase in surface energy due to formation of amorphous regions. Untreated and recrystallized materials have similar surface energies at low surface coverages but show clear differences in energy distribution.

Keywords Inverse Gas Chromatography; active site theory; lactose; milling; surface energy; heterogeneity

INTRODUCTION

The processing and performance of solid formulations depends strongly on the interaction at the interface of the different compounds in the blend (Zeng, Martin & Marriot, 2001). This interaction is affected by the surface heterogeneity. Surface heterogeneity can be attributable to porosity, surface roughness (rugosity), and distribution of the energy on the surface (Gregg & Sing, 1982; Rudzinski & Everett, 1992; Thielmann & Pearse, 2002). The latter is related to a variation in surface energy of different active sites on the surface of a solid.

Young and Price suggested that the existence of different active sites on a solid can have an impact on the aerosolization performance of dry powder inhalation (DPI) formulations (Young & Price, 2006) with lactose as a carrier. α-Lactose monohydrate is used in such formulations to overcome the high cohesiveness of the micronized drug. The authors showed by colloid probe microscopy that there exists a wide variation in energy distribution—even for unprocessed standard lactose that consisted mostly of α-Lactose monohydrate. For instance, in a formulation of different lactose grades with salbutamol sulphate there is a large variation in fine particle fraction (FPF). Especially in low dose drug systems there is initially a reduction in FPF despite an increase in loaded dose due to the strong adhesion of fine drug particles to the high energy sites of the lactose carrier. Generally, active sites of enhanced energy can be amorphous (Chan, 2006; Ticehurst, York, Rowe & Dwivedi, 1996) or certain face-specific regions (Heng, Thielmann, & Williams, 2006; Larhib, Zeng & Martin, 1999). If the loaded dose is increased further the FPF increases as these high energy sites are "saturated." In this case there should be a critical surface energy where the drug remains on the carrier. This would be an "upper limit" for the surface energy above which the drug-carrier interaction would be too strong.

However, there also must be a "lower limit" of drug-excipient adhesion since certain process steps such as mixing or capsule filling require a good content uniformity. Such uniformity can only be achieved if the drug-excipient interaction is reasonably strong compared to the drug-drug cohesion (Begat & Price, 2004; Thielman, Naderi, Young, & Traini, 2006).

From the above it is obvious that the distribution of the surface energy is highly relevant for an understanding of processing and formulation performance. In this paper a new method is described for the determination of the surface energy distribution by Inverse Gas Chromatography (IGC). The method is applied to investigate the surface heterogeneity of an untreated standard lactose, milled, and recrystallized lactose in combination with other techniques.

Address correspondence to Frank Thielmann, Surface Measurement Systems UK, 5 Wharfside, Rosemount Road, London HA0 4PE, UK. E-mail: frank_thielmann@yahoo.co.uk

METHOD

IGC is a well-known method for the determination of surface energetics and has been applied in various studies on pharmaceutical materials addressing issues such as flowability (Feeley, York & Sumby, 1998), milling (Heng et al., 2006; York, Ticehurst, & Osborn, 1998), and content uniformity (Galligan, Buckton, & Burrows, 2000). A good overview of various applications can be found in reference (Grimsey, Feeley & York, 2002) and (Domingue, Burnett & Thielmann, 2003). IGC inverts the roles of the stationary and mobile phase as found in conventional gas chromatography since a solid of unknown properties is packed into a column and probed with known vapors to determine its physico-chemical characteristics. This has various advantages over conventional wettability techniques since it avoids changes in the sample morphology as well as problems with porosity and bulk absorption. However, in the past IGC was mainly used in the infinite dilution range. This involves the injection of very small concentrations of vapors and an interaction with high-energy sites on the material surface takes place.

The surface energy can be divided into a dispersive and a specific contribution. The former is due to Lifshitz-van der Waals interactions and the latter is related to electrostatic forces (Oss & Good, 1989). The dispersive surface energy can be determined directly by an injection of a range of alkanes while the specific contribution can only be indirectly assessed through the determination of the specific free energies of various polar probes. The retention time of each injected probe vapor depends on the strength of interaction with the sample surface: the stronger the interaction, the higher the retention time. The gross retention time, t_R obtained from the maximum (or the centre of mass) of the eluted peak has to be corrected for the deadtime, t_0 of the system. The deadtime is the time a non-interacting probe takes to pass through the IGC system. If the deadtime is subtracted the net retention time is obtained and can be transformed into the retention volume, V_N via Eq. (1).

$$V_N = j/m \cdot F \cdot (t_R - t_0) \cdot \frac{T}{273.15} \tag{1}$$

where T is the column temperature, m is the sample mass, F is the exit flow rate at 1 atm, and 273.15 K. j is the James-Martin correction factor, which corrects the retention time for the pressure drop in the column bed. The net retention volume of each alkane injection is related to the dispersive surface energy, γ_S^D via Eq. (2).

$$RT \ln V_N = 2N_A(\gamma_S^D)^{1/2} a(\gamma_L^D)^{1/2} + const. \tag{2}$$

In Eq. (2) N_A is the Avogadro constant, R is the gas constant, γ_L^D is the dispersive surface tension of the probe, and a its cross sectional area. If the term $RTlnV_R^0$ for a range of injected alkanes is plotted versus $a(\gamma_L^D)^{1/2}$ a straight line results and the dispersive surface energy can be calculated from the slope of the corresponding linear fit (Schultz, Lavielle & Martin, 1987). When in addition polar probes are injected data points will be located above the alkane line if plotted in the same coordinates. The vertical distance between each point of a polar probe and the alkane line is a direct measure for the specific contribution of the free energy, ΔG^{sp} (Schultz et al., 1987). With the knowledge of the specific free energy an acid-base concept such as the Gutmann or Good-van Oss theory could be applied to obtain acid and base numbers for the solid surface (Mukhopadhyay & Schrieber, 1995) or specific surface energies (Goss, 1997).

Although infinite dilution conditions are advantageous in terms of an increased measurement sensitivity (Thielmann, 2004) it limits the investigation of the surface to high-energy sites. For a study of the entire surface less energetic sites need to be taken into account. This can be achieved by an increase in vapor partial pressure to finite concentration conditions. For a study of the surface heterogeneity vapors are injected at different concentrations. There are numerous different approaches in literature for the mathematical treatment of the results of such experiments. An overview can be found in reference (Rudzinski & Everett, 1992). However, the results are usually expressed as adsorption potential (Jaroniec, Gadkarcc, & Choma, 1996) or adsorption energy distribution (Balard, 1997). In the former method retention times/volumes of a probe vapor are determined at different vapor partial pressures. A plot of the retention volume versus the partial pressure results in a curve that represents the first derivative of the sorption isotherm. A detailed description of the determination of adsorption isotherms from finite concentration IGC measurements can be found in (Cremer & Huber, 1962). In principle two methods can be distinguished for the isotherm calculation: the Peak Maximum (PeakMax) and Elution of a Characteristic Point (ECP) method. For the PeakMax method different concentrations (partial pressures) of a probe vapor are measured and the retention volume and equilibrium partial pressure in the maximum are calculated for each single injection concentration. In the case of the ECP method one assumes that each maximum of individual peaks from single injections coincides with the rear of a peak produced by the highest injection concentration. For this reason the isotherm can be calculated from just one peak. However, this assumes that the curvature of the rear of the peak is entirely due to adsorption/desorption effects. In reality there is also a contribution from the gas phase diffusion (Cremer & Huber, 1962). This diffusion effect can be partially eliminated by applying the correction according to Bachmann, Bechtold, and Cremer (1962), so that isotherms from PeakMax and ECP calculations coincide.

In order to obtain the adsorption potential distribution function the partial pressures of the sorption isotherm are converted into a sorption potential, A by Eq (3).

$$A = R \cdot T \cdot \ln\left(\frac{po}{p}\right) \tag{3}$$

where *p* is the partial pressure, *po* the saturation pressure, *R* the gas constant, and *T* the column temperature. The distribution parameter, Φ can be obtained from the first derivative of the sorbed amount, *n* with the sorption potential *A* as shown in Eq. (4).

$$\Phi = -\frac{dn}{dA} \tag{4}$$

The distribution function can be normalized by dividing through the monolayer capacity n_m.

Although this approach is very valuable it suffers from the fact that the adsorption potential as well as adsorption energy distributions are probe molecule dependent, meaning the results change depending on the vapors used in the experiment. For this reason it would be preferable to determine the distribution of the *surface energy* since this parameter is a sole property of the material surface. Unfortunately, the calculation used at infinite dilution cannot simply be extended to the finite concentration case due to the non-linear shape of the adsorption isotherm in this region. In the non-linear part of the isotherm the retention volume depends on the surface coverage. Probe molecules injected by pulse chromatography adsorb usually at different surface coverages since it is difficult to predict the equilibrium partial pressure in this discontinuous adsorption method. Bogillo, Shkilev, and Voclkel (1996) suggested a method that allows for a calculation of the adsorption energy distribution directly from the retention volumes of finite concentration measurements. The adsorption energy function could then be used to estimate an average dispersive surface energy as well as the specific free energies for various polar probes. However, this method did not provide the distribution of the surface and free energies.

To determine the surface energy distribution the retention volumes obtained from measurements at different concentrations must be corrected for their surface coverage. This can be achieved by assuming that alkanes as well as weakly polar vapors adsorb in a Type II adsorption mechanism (Thielmannn & Baumgarten, 2000). In this case the isotherms show a "knee-shape" at low partial pressures which is associated with the formation of a (statistical) monolayer before multilayer adsorption occurs. This is usually a valid assumption if the vapor-vapor interactions are significantly lower than the vapor-solid interactions (van den Berg & Bruin, 1981). In this case the monolayer capacity of the surface can be determined directly from the isotherm of each probe vapor by applying the BET equation, Eq. (5) or estimated if the BET surface area is known from separate experiments, e.g., with nitrogen adsorption techniques.

$$n = \frac{n_m \cdot c \cdot p/p_0}{(1-p/p_0)\cdot(1-(1-c)\cdot p/p_0)} \tag{5}$$

In this equation *c* is the BET constant and all other constants have the same meaning as above.

With the knowledge of the monolayer capacity the surface coverage Θ can be calculated according to Eq. (6) as suggested by Langmuir (1918).

$$\Theta = n / n_m \tag{6}$$

The retention volume can now be obtained for different surface coverages by differentiation of the isotherm. To facilitate the differentiation and to generate more data points, especially in case of a peak maximum analysis, the isotherms have been fitted using a linear combination between the Henry and BET equation as shown in Eq. (7).

$$n = C\cdot p/p_0 + \frac{A\cdot B\cdot p/p_0}{(1-p/p_0)\cdot(1-(1-B)\cdot p/p_0)} \tag{7}$$

This simple extended BET equation gives remarkably good fits in the experience of the authors, especially if the isotherms are predominately of Type II. It should be pointed out here that the linear combination normally requires two "weighing" factors. However, in this case they are already included in the constants for A, B, and C. This is the reason why the classical BET and Henry constants have been replaced as they do not have the same physical meaning in Eq. (7).

In theory it would be also possible to analyze the retention volume curves directly and to avoid the extra step of an isotherm calculation. However, for the results obtained in this paper the analytical description of a Type II isotherm is much simpler and more accurate than that of the retention volume curve.

If now the retention volumes at the same surface coverages are compared Eq. (2) can be applied and the dispersive surface energies can be calculated as described above for each surface coverage. In addition the specific free energies for each coverage can be obtained using the same approach. Consequently, acid-base numbers could also be obtained as a function of surface coverage. However, in this study only ethanol was used to obtain a measure for the affinity of the surface to an amphoteric and hydrophilic acid-base probe vapor.

EXPERIMENTAL

Materials

α-Lactose monohydrate was obtained from Acros Organics, Loughborough, UK, ACS grade (CAS 5989-81-1). The "as received" lactose material (as well as all other materials after treatment) were sieved using ASTM Test Sieves (Endecotts, Chelmsford, UK) and the sieve fraction 63–90 μm was collected for further experiments. The milled sample has been generated by grinding 20 g of the initial material (which will be referred to as "untreated lactose" in the following sections) using a Minigrinder (Micromark, London, UK). The grinding time was 3 min. After sieving the material was collected and

will be referred to as "milled lactose". A few grams of the milled sample were placed in a petri dish and put into a desiccator together with a petri dish filled with water. The desiccator was sealed and the sample was exposed to this humid environment for 24 h in order to recrystallize any amorphous material which may have been present after milling. The sample was then dried in an oven at 40°C for 12 h to remove the physisorbed water. Finally, the material was sieved as described above and will be referred to as "recrystallized lactose".

Particle Size Analysis

Particle size analysis was carried out after sieving to confirm a comparable size range for all samples. Particle size distribution was determined using a laser light scattering based particle size analyzer (Malvern Mastersizer 2000, Malvern Instruments, Worcestershine, UK) in accordance with ISO 13320 (using the Mie theory) fitted with a small volume sample dispersion unit. A small amount (< 0.2 g) of sample was dispersed into 200 mL of acetone in a large beaker with a stirring rate of 2000 rpm used, providing for a thorough mixing of the particles in suspension. The suspension was allowed to fill the glass cuvette placed in the laser path of the instrument. Six measurements were obtained for each sample.

Dynamic Vapor Sorption (DVS)

Dynamic gravimetric vapor sorption was used for the determination of the amorphous content of the lactose samples. Experiments were carried out with a DVS Advantage instrument (Surface Measurement Systems Ltd., London, UK). The amorphous content has been determined by the method of Mackin, Zanon, and Park (2002). In this approach the solvent vapor sorption is measured below the vapor pressure at which crystallization would occur. Then the partial pressure is increased above this point and subsequently reduced back to the original vapor pressure where the vapor sorption is measured again. In the current investigation water has been used as the crystallization solvent. The adsorption of water has been determined at 20% relative humidity (RH) and 25°C. The sample was crystallized at 95% RH and then the humidity reduced to 20%. The difference in the uptake at 20% RH is used as a measure for the amorphous content. Experiments have been carried out in duplicate on all three samples.

Optical Imaging (Microscopy)

A visual comparison of the untreated samples with the samples after milling and recrystallization was carried out by obtaining photomicrographs of the particle surfaces using an Olympus BX51M optical microscope (Olympus, Japan) fitted with a DP70 camera. To enhance the depth focus, the Extended Focal Imaging (EFI) module was used by taking a series of single images at various focus levels. These images were then compiled into a composite image using an ANALYSIS FIVE software (Olympus), resulting in a sharp focus for the whole image.

Inverse Gas Chromatography (IGC)

IGC experiments were carried out using an *iGC 2000* (Surface Measurement Systems Ltd., London, UK) with a flame ionisation detector. The lactose samples were packed into standard columns (30 × 0.3cm ID) using a tapping machine from the same supplier. Columns were filled with 2–3 g of material and then conditioned in situ for 2 h at 30°C to remove physisorbed water. Measurements were performed with a range of alkanes (decane, nonane, octane, heptane) and ethanol as a polar probe, all supplied by Aldrich (Gillingham) in HPLC grade. Injections were made in duplicate using a range of different vapor concentrations via a vapor sample loop with 0.25 mL volume at 30°C and 10 mL/min flow rate of the helium carrier gas. For the untreated lactose a second column was packed to investigate sample-to-sample variation.

RESULTS AND DISCUSSIONS

Particle Size Analysis

Figure 1 shows the particle size distributions obtained for all three samples. The mean particle size (d 0.5) was 73.85 μm for the untreated sample, 56.11 μm for the milled material, and 76.53 μm for the recrystallized sample. All three samples show a rather uniform distribution. However, despite the sieving a small shoulder is visible at lower particle sizes as well as another small shoulder for the recrystallized material at high particle sizes. The former could be explained by agglomeration of smaller fines that are strongly attached to other fines or bigger particles and cannot be separated by the sieving procedure. The reason for the shoulder at higher particle size for the recrystallized material is less obvious but might be related to fracturing and re-agglomeration during sieving.

DVS Measurements

The amorphous content of the three samples was determined by water sorption as described above. Figure 2 demonstrates the method by means of the milled lactose. The diagram shows the uptake at 20% RH before and after exposure to 95% RH. From the change in weight at 95% RH it can be clearly seen that the sample recrystallizes during the humidity exposure suggesting that the milling procedure introduced amorphous regions on the surface. The difference before and after exposure yields to 0.023% while the reference amorphous sample (obtained by spray-drying) with 100% amorphous content shows a differences in uptake at 20% RH of 0.080%. Therefore, an amorphous content of 1.25% results for the milled sample. The unmilled sample gives an amorphous content of 0.2% while the value for the recrystallized material was well below 0.1% which represents the detection limit of the approach for this system.

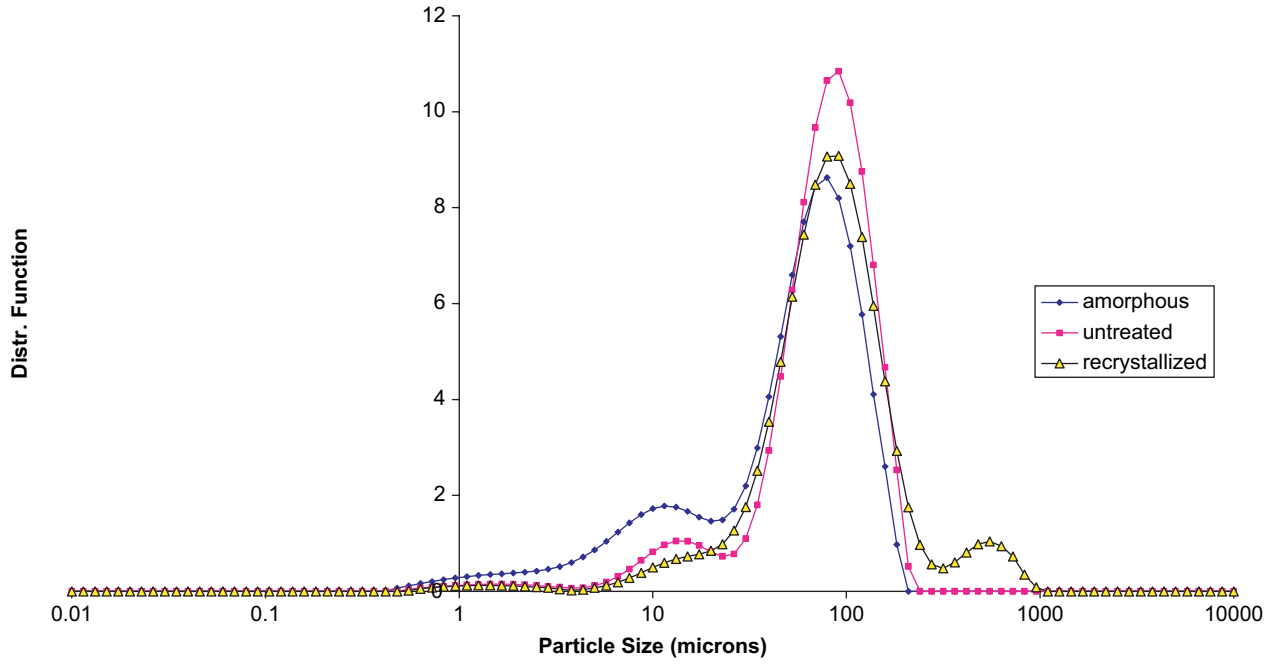

FIGURE 1. Particle size distribution for all three lactose samples measured by laser diffraction.

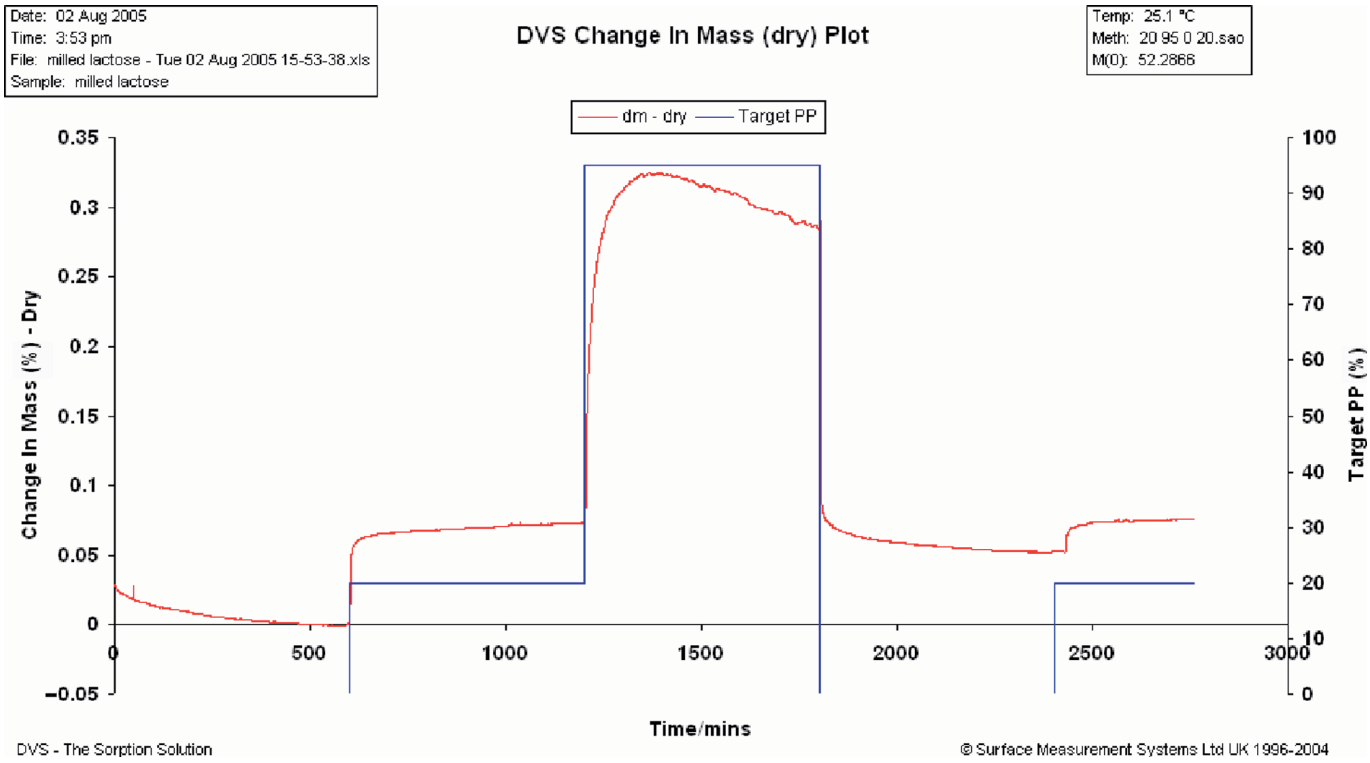

FIGURE 2. DVS humidity change and balance response for milled lactose at 298 K.

Optical Imaging

The optical images obtained for the three samples are shown in Figures 3a–c. The figures differ in surface morphology. The untreated sample in Figure 3a shows a certain degree of surface roughness which is even more significant for the milled material in Figure 3b. In contrast, the recrystallized sample in Figure 3c

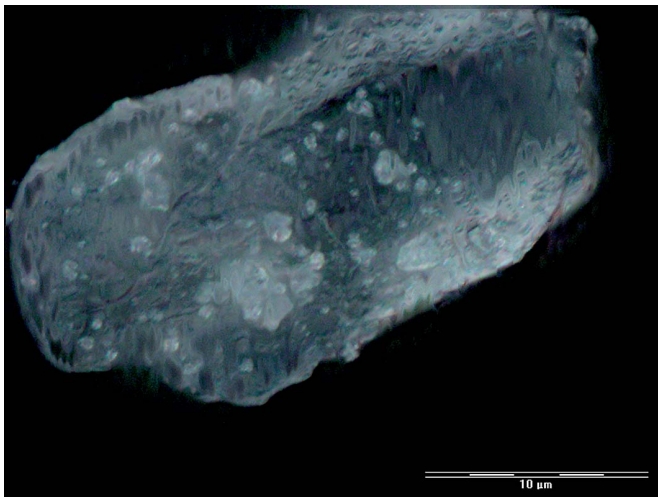

FIGURE 3a. Optical mlicroscope image of untreated lactose.

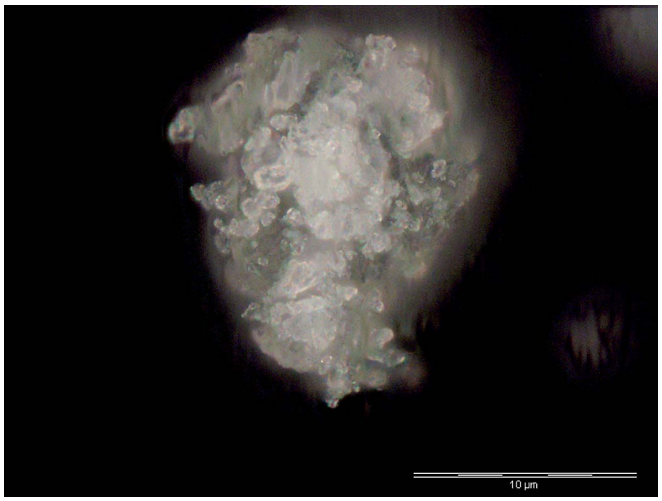

FIGURE 3b. Optical microscope image of milled lactose.

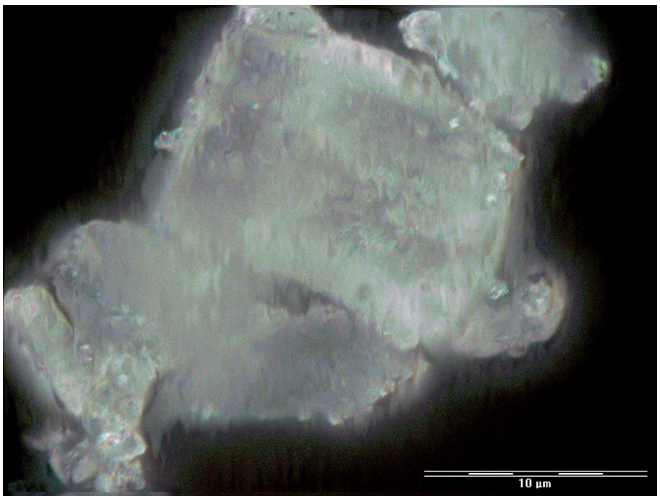

FIGURE 3c. Optical microscope image of recrystallized lactose.

appears to have a relatively smooth surface. Since experiments were repeated in various different regions of the sample the authors would consider these images as representative. However, AFM or SEM experiments could provide more detailed information on surface roughness and confirm the observations of this study.

IGC Measurements

Sorption isotherms were calculated according to the ECP and PeakMax method as described above. Figure 4 shows the heptane isotherms (as an example for an alkane) obtained from ECP (before and after diffusion correction) and PeakMax analysis for the untreated lactose.

There is generally a good agreement between the PeakMax and ECP method with diffusion correction (keeping in mind the small changes on the *y*-axis). Since the ECP analysis requires only the injection of one (maximum) partial pressure for each probe vapor this method would be beneficial from an experimental point of view due to the dramatic reduction of measurement time compared to the PeakMax method where an injection has to be made for each data point. However, in the authors' experience isotherms obtained from PeakMax analysis are more accurate and give more reproducible values for most pharmaceutical materials. This is due to the fact that the ECP analysis assumes a distinct Type II adsorption mechanism and therefore a relatively strong vapor-solid interaction. However, this is not always the case, especially if solids have a lower-energy surface or the probe vapors have a strong intermolecular interaction, for example due to hydrogen bonding. In that case PeakMax measurements give better results as the analysis does not assume any specific adsorption mechanism. A more detailed consideration of isotherm types and adsorption mechanism has been carried out in reference (Thielmann & Burnett, 2002).

Figure 5 shows a comparison of the heptane sorption isotherms for the three different lactose samples as well as a repeat measurement for the unmilled lactose. These isotherms have been obtained from ECP analysis of the peak resulting from the highest injection concentration.

It can be seen that the experiment-to-experiment reproducibility is excellent and deviations are small compared to the differences observed between the three types of lactose. The fit parameters based on the extended BET equation described above are summarised in Table 1. Although one might argue the physical meaning of the constants the regression coefficients shown in Table 1 are 0.999 or better. This confirms that Eq. (7) allows for a very accurate description of the isotherms measured.

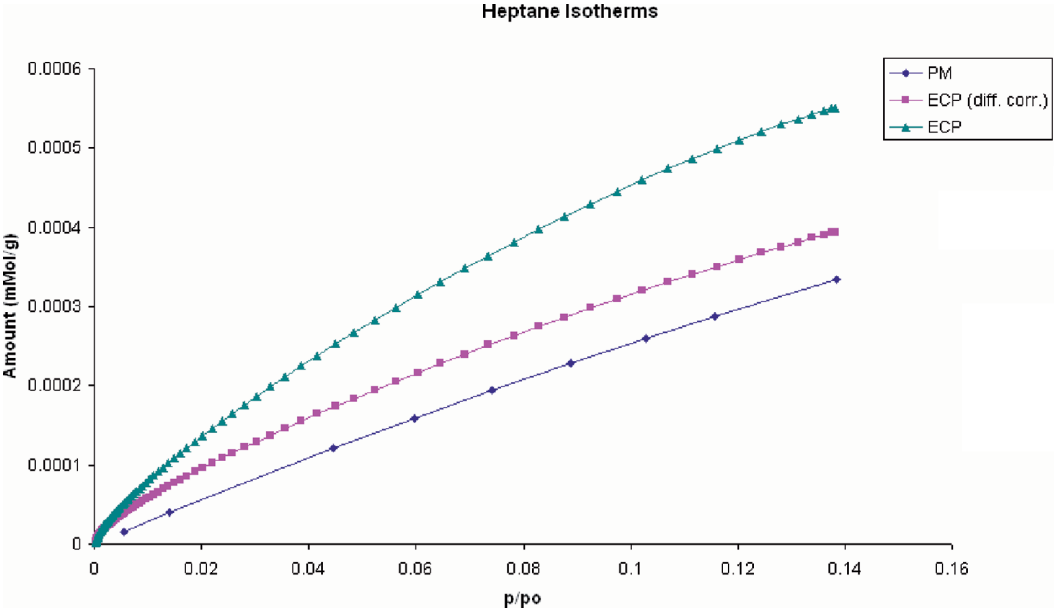

FIGURE 4. PeakMax and ECP isotherms for heptane (amount adsorbed *n* as a function of partial pressure p/po) on untreated lactose at 303 K.

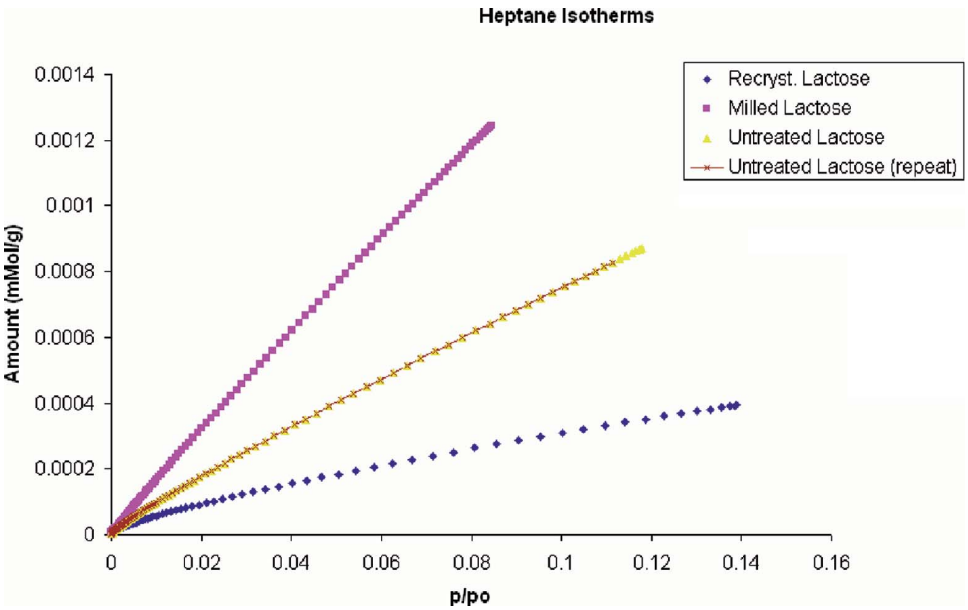

FIGURE 5. Heptane isotherms (amount adsorbed *n* as a function of partial pressure p/po) on all three lactose samples at 303 K.

TABLE 1
Fit Parameter and Regression Coefficients From the Fits of the Extended BET Equation to Heptane Isotherms for the Three Lactose Samples

Sample	a	b	c	Regr. Coeff.
Untreated Lactose	0.001539	5.488474	0.001121	0.999305
Milled Lactose	0.003688	4.291087	0.001249	0.999882
Recrystallized Lactose	0.000932	3.703794	–0.00049	0.999958

TABLE 2
BET Surface Areas of the Three Lactose Samples Determined From the Heptane Isotherms Obtained by IGC Experiments at 303 K

Sample	S_{BET} (m^2/g)
Untreated Lactose	0.80 ± 0.03
Milled Lactose	1.57 ± 0.05
Recrystallized Lactose	0.22 ± 0.02

With the knowledge of the fit parameters the retention volumes can now be calculated based on the first derivative of the extended BET equation. The corresponding surface coverages can be determined from the amount adsorbed and the monolayer capacities for each probe. The surface areas that are required for the calculation of the monolayer capacity are summarised in Table 2 for the three lactose samples. The numbers for the surface areas show bigger differences than one may expect based on similar particle size distributions. However, these differences can be easily explained by the variation in roughness between the three samples which is supported by the differences observed in Figures 3a–c.

Figures 6 to 8 show a comparison of the retention volumes as a function of surface coverage for all vapor probes injected. As one would expect the retention volume generally decreases with increasing surface coverage. Moreover, in all three cases the heavier alkanes show higher retention volumes. The retention volumes for ethanol are relatively high at low coverages, suggesting a strong interaction but decrease steeply at higher coverages. When the curves for the three samples are compared untreated and milled lactose show a much steeper decline in retention volume with surface coverage than the recrystallized sample.

From the retention volumes the dispersive surface energy as well as the specific free energy can now be calculated for each point at the same surface coverage using Eq. (6). The resulting graphs are illustrated in Figure 9 for the dispersive surface energy and in Figure 10 for the specific free energy of ethanol.

As expected from the retention volume curves the surface and free energy decrease with increasing surface coverage since more and more less active sites will contribute to the overall interaction.

It can be seen from Figure 9 that the dispersive contribution to the surface energy at zero coverage (corresponding to infinite dilution conditions) is the highest for the milled sample (around 53 mJ/m^2) while the value for the other two samples is very similar (around 42 mJ/m^2 at zero coverage). This agrees well with results from infinite dilution measurements published in the literature for fairly crystalline in the latter and relatively amorphous materials in the former case (Planinsek, Zadnik & Rozman, 2003; Ticehurst et al., 1996). Milling can introduce significant levels of amorphous material (Mackin et al., 2002; Saleki-Gerhardt, Ahlneck, & Zograffi, 1994) causing not only an increase in surface area but also in surface energy. Despite having a comparable dispersive surface energy

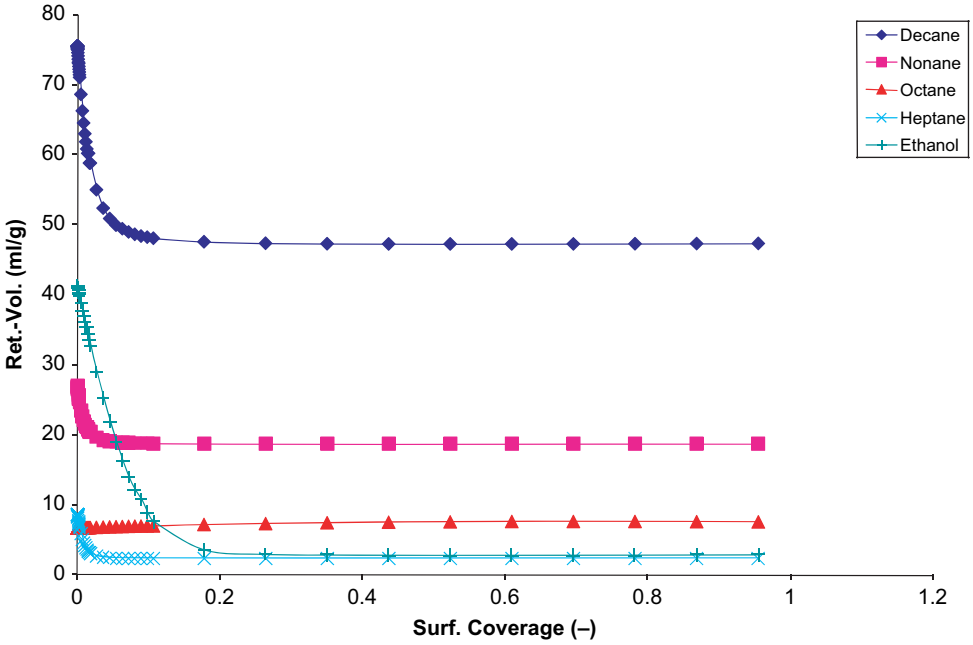

FIGURE 6. Change in retention volume with surface coverage for untreated lactose.

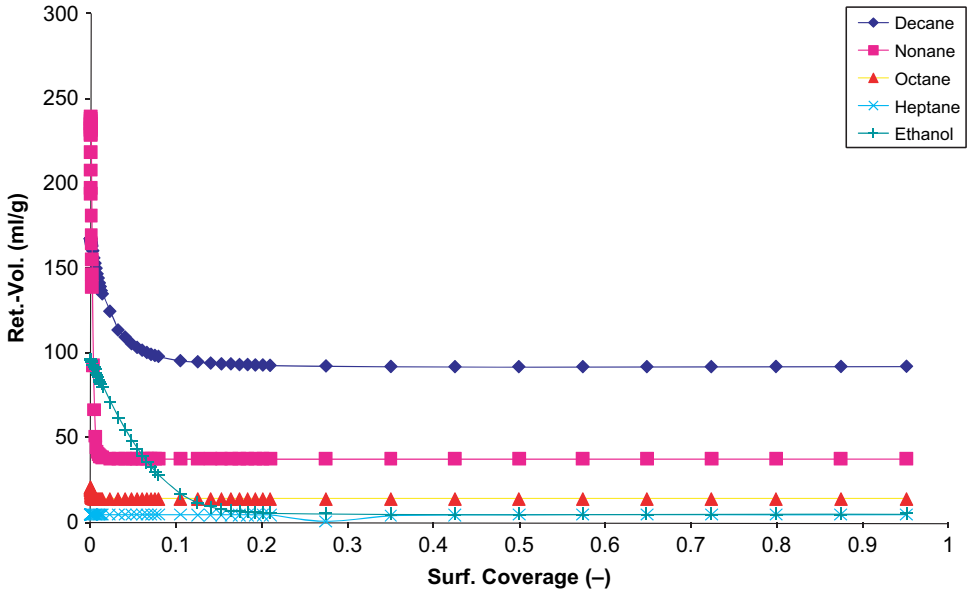

FIGURE 7. Change in retention volume with surface coverage for milled lactose.

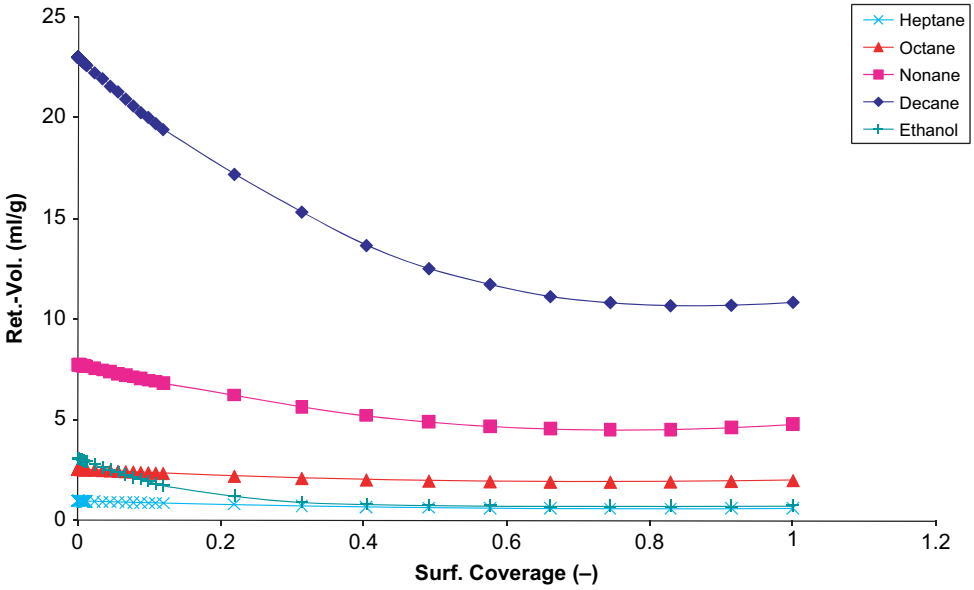

FIGURE 8. Change in retention volume with surface coverage for recrystallized lactose.

at zero coverage the curves for the recrystallized and untreated material show a different progression at higher surface coverages. It is also noticeable that the milled and untreated samples have nearly reached a constant surface energy level below 10% coverage while the curve for the recrystallized material levels off well above 70% coverage. This suggests that the energy distribution is more homogenous for the recrystallized samples.

The specific free energies for ethanol show slightly different trends. At zero coverage the milled sample shows a higher value than the recrystallized sample. Surprisingly, the untreated material has a higher specific free energy at zero coverage than the milled sample. With increasing surface coverage the milled and untreated sample exhibit a similar steep decrease in free energy. This could be related to the very small

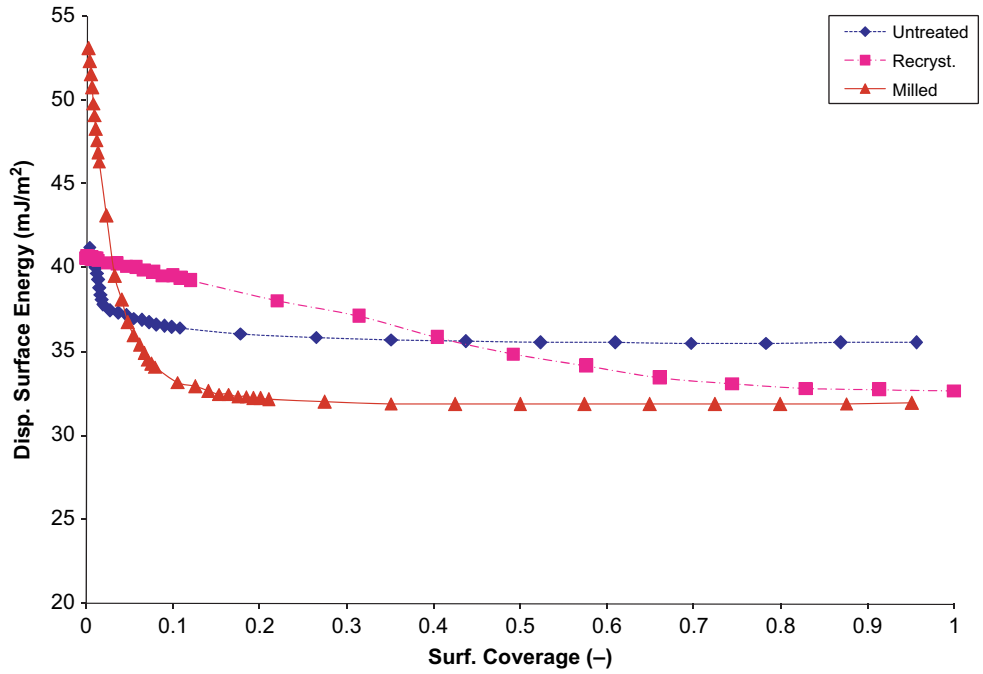

FIGURE 9. Change in dispersive surface energy with surface coverage for all three lactose samples.

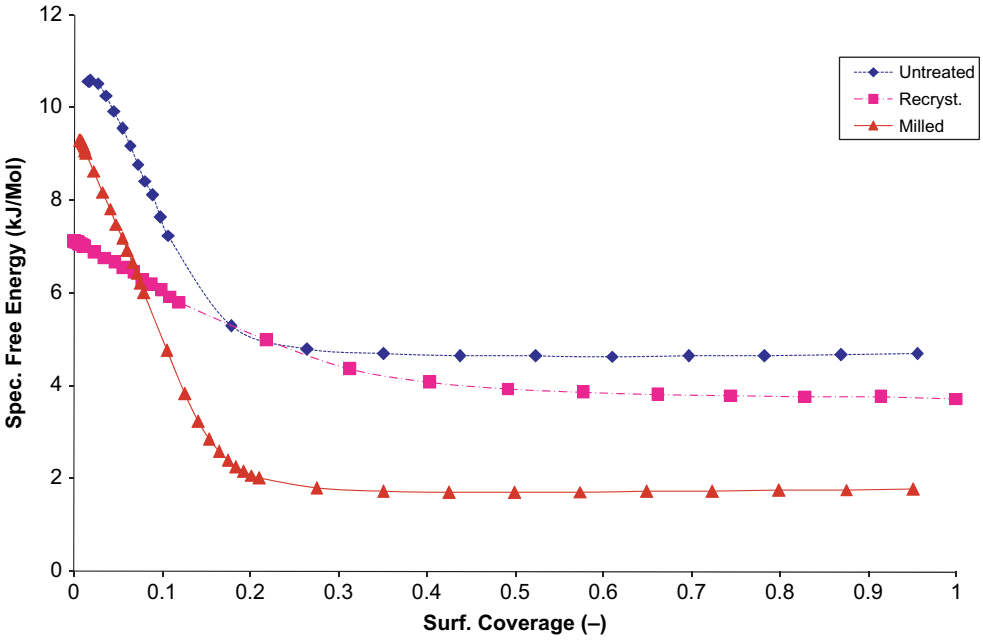

FIGURE 10. Change in specific free energy of ethanol with surface coverage for all three lactose samples.

but detectable amorphous regions on the surface of the untreated sample.

It is possible to obtain a rough idea about the differential energy distribution without any modelling or other assumptions by point-to-point integration of the curves in Figures 9 and 10. The area increments can then be transformed into histograms reflecting an energy distribution. The resulting diagrams are displayed in Figure 11a–c for the dispersive surface energy and in Figure 12a–c for the specific free energy of ethanol.

When the dispersive surface energy distributions of the lactose samples are compared in Figures 11a–c the histograms show significant differences in the profiles. The values for the

(a) Untreated

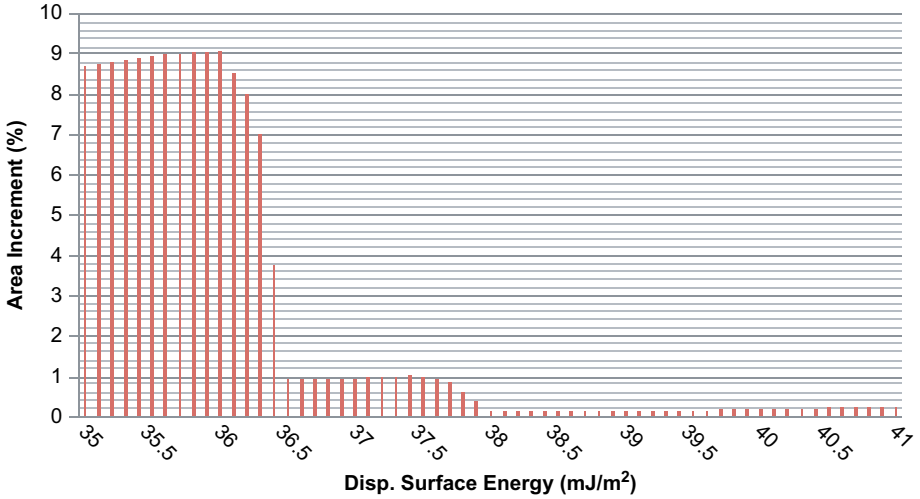

(b) Recrystallized

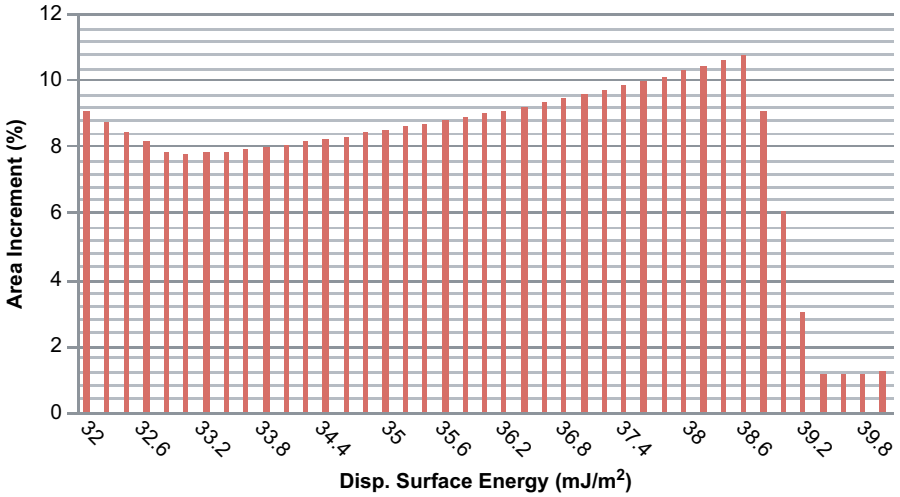

(c) Milled

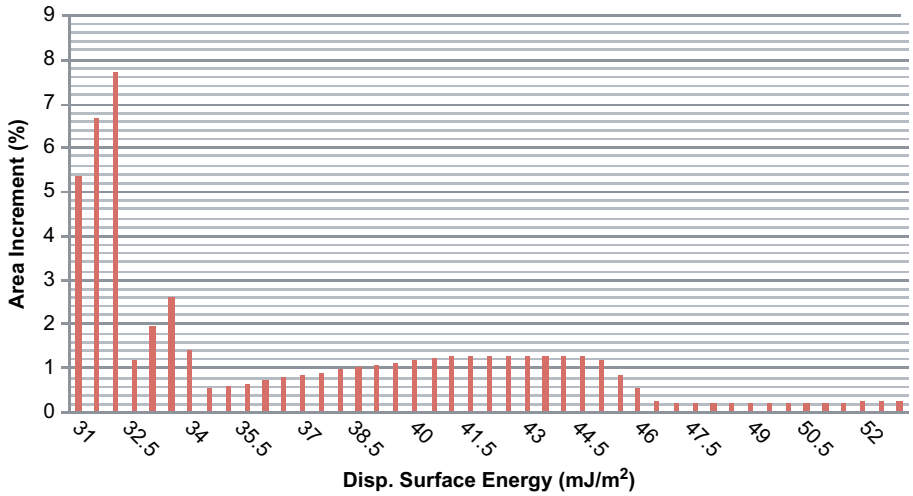

FIGURE 11. Distribution of surface energy for all three lactose samples.

(a) Untreated

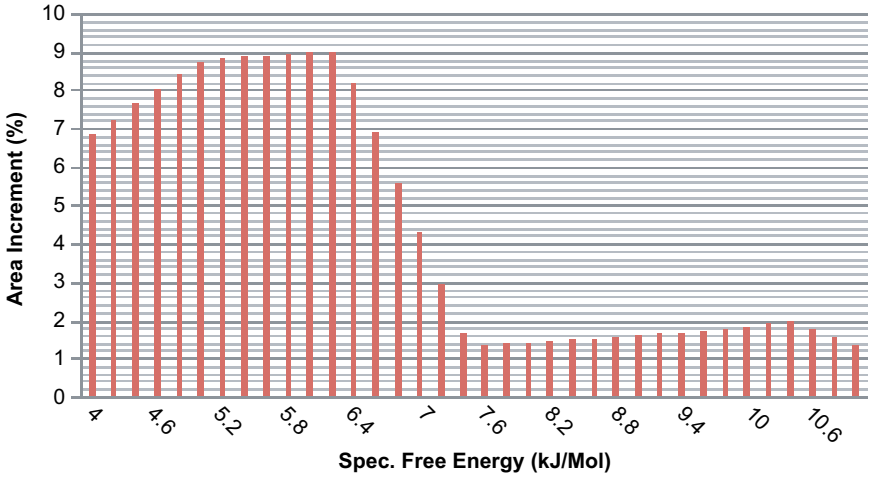

(b) Recrystallized

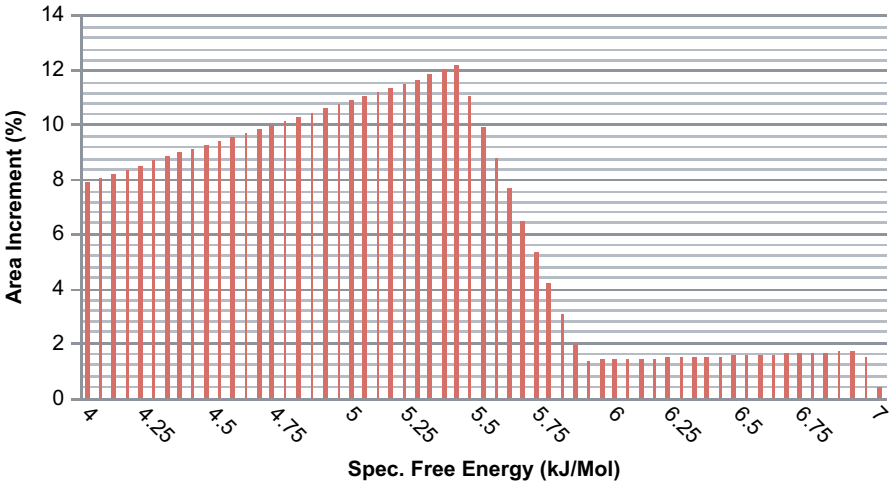

(c) Milled

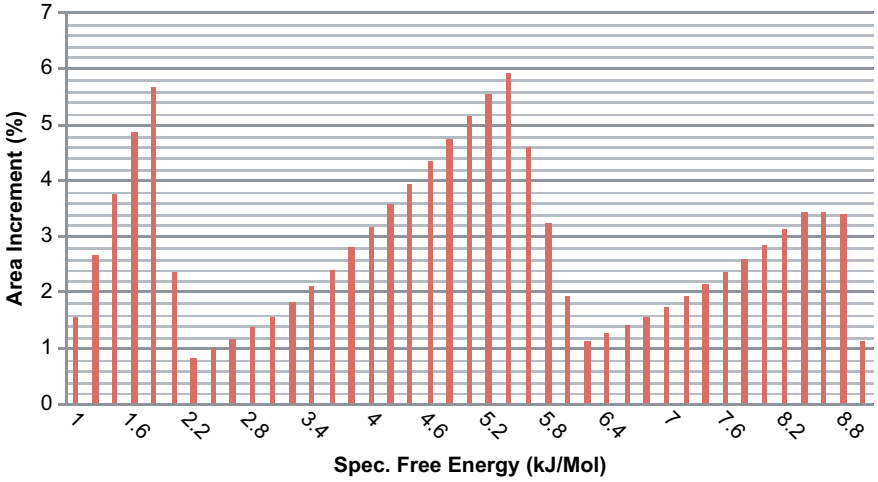

FIGURE 12. Distribution of specific free energy of ethanol for all three lactose samples.

milled material are shifted to high surface energies compared to the other two samples. The profile of the milled material also reveals three distinct maxima around 31, 33 mJ/m^2 and a broad peak at 40 mJ/m^2. When the recrystallized and untreated sample are compared it is obvious that the recrystallized material shows a broad but fairly even distribution between 32 and 38 mJ/m^2 while the untreated sample shows a clear peak around 35 and a shoulder around 37 mJ/m^2. Since there are no significant differences in the amorphous content of the recrystallized and untreated lactose it can be assumed that the variations in peak position and width are related to differences in the composition of the crystalline form. Those variations could be explained by impurities or variation in anomeric composition. Lactose can crystallize not only as α-monohydrate but also in an anhydrous β and α form as well as in mixed forms. The anomeric composition can have a strong influence on surface energies and formulation performance (Thielmann et al., 2006).

A comparison of the histograms for the ethanol specific free energies in Figure 12a–c shows a different picture. All three curves reveal a distinct peak around 5.2 kJ/Mol. The milled sample also has an additional peak around 8.5 and at 1.5 kJ/Mol. It could be speculated whether the peak at 8.5 kJ/Mol is due to the amorphous contributions. However, further studies by XRD and spectroscopic methods would be required to clarify the observations in this paper.

CONCLUSIONS

Three different lactose samples have been investigated: an untreated, a milled and a recrystallized material. Sieving and particle size analysis were applied to ensure similar particle size distributions. IGC measurements at finite concentration allowed for a study of the distribution of the dispersive surface energy as well as an investigation of the distribution of the specific free energy of ethanol. Although untreated and recrystallized lactose showed a similar dispersive surface energy at infinite dilution the energy distributions for the two samples are quite different. For the milled material there is a shift in the energy distribution of dispersive as well as specific component to higher values, compared to the other two samples. In combination with DVS amorphous content results this suggests that the milled sample has a significant amorphous content while the amorphous content of the untreated and recrystallized sample is extremely small. The differences observed between the untreated and recrystallized material were therefore associated with other factors such as variations in the samples' anomeric compositions or impurities. The study has demonstrated the potential of this IGC finite concentration method to provide an improved understanding of changes in surface energy and energy distribution observed during processing on the surface of a sample. As the next step a correlation with formulation properties and in vitro behaviour shall be carried out. Of course, the approach should also be valuable in formulation development in other areas such as oral solid dosage forms.

ACKNOWLEDGMENTS

The authors would like to thank Dr Jeffrey Brum and Dr Ted Sokoloski of GlaxoSmithKline, Collegeville as well as Dr Daryl Williams of Imperial College, London, UK for various fruitful discussions.

REFERENCES

Bachmann, L., Bechtold, E., & Cremer, E. (1962). Gas-chromatographic separation of ortho and para hydrogen on molecular sieves. *J. Catal.*, *1*, 113.

Balard, H. (1997). Estimation of the surface energetic heterogeneity of a solid by inverse GC. *Langmuir*, *13*, 1260.

Begat, P., & Price, R. (2004). The cohesive-adhesive balances in dry powder inhaler formulations: direct quantification by atomic force microspcopy. *Pharm. Res*., *21*, 1591.

Bogillo, V., Shkilev, V., & Voelkel, A. (1996). Determination of surface free energy components for heterogeneous solids by inverse GC. *J. Mater. Chem.*, *8*, 1953.

Chan, H-K. (2006). Dry powder aerosol delivery systems: Current and future research directions. *J. Aerosol Med*., *19*, 21.

Cremer, E., & Huber, H. (1962). Measurement of adsorption isotherms by means of high temperature elution gas chromatography. *Proc. Intern. Symp. Gas Chrom.*, *3*, 169.

Domingue, J., Burnett, D., & Thielmann, F. (2003). Using inverse GC to investigate process-related changes in surface and bulk properties of pharmaceutical materials. *Amer. Lab*., *7*, 32.

Feeley, J., York, P., & Sumby, B. (1998). Determination of surface properties and flow characteristics of salbutamol sulphate, before and after micronisation. *Int. J. Pharm*., *172*, 89.

Galligan, C., Buckton, G., & Burrows, R. (2000). Investigation of a possible link between solid surface energy measured by inverse GC and powder mix uniformity. Pharm. Sci. (Suppl.) 2(4).

Goss, K. (1997). Considerations about adsorption of organic molecules from the gas phase to surfaces. *J. Coll. Interf. Sci*., *190*, 241.

Gregg, S., & Sing, K. (1982). *Adsorption, surface area, and porosity.* San Diego, California: Academic Press.

Grimsey, I., Feeley, J., & York, P. (2002) Analysis of the surface energy of pharmaceutical powders by inverse GC. *J. Pharm. Sci*., *91*, 571.

Heng, J., Thielmann, F., & Williams, D. (2006). The effects of milling on the surface properties of form I paracetamol crystals. *Pharm. Res*., *23*, 1918.

Jaroniec, M., Gadkaree, K., & Choma, J. (1996). Relation between adsorption potential distribution and pore volume distribution for microporous carbons. *Coll. Surf. A*, *118*, 203.

Langmuir, J. (1918). The adsorption of gases on plane surfaces of glass, mica, and platinum. *J. Am. Chem. Soc.*, *40*, 1361.

Larhib, H., Zeng, X., & Martin, G. (1999). The use of different grades of lactose as carrier for aerosolised salbutamol sulphate. *Int. J. Pharm*., *191*, 1.

Mackin, L., Zanon, R., & Park, J. (2002). Quantification of low levels of amorphous content in micronised active batches using dynamic vapor sorption and isothermal microcalorimetry. *Int. J. Pharm*., *231*, 227.

Mukhopadhyay, P., & Schreiber, H. (1995). Aspects of acid-base interactions and use of inverse GC. *Coll. Surf. A*, *100*, 47.

Planinsek, O., Zadnik, J., & Rozman, S. (2003). Influence of inverse GC measurement conditions on surface energy parameters of lactose monohydrate. *Int. J. Pharm*., *256*, 17.

Rudzinski, W., & Everett, D. (1992). *Adsorption of gases on heterogeneous surfaces*. San Diego, California: Academic Press.

Saleki-Gerhardt, A., Ahlneck, C., & Zografi, G. (1994). Assessment of disorder in crystalline solids. *Int. J. Pharm.*, *101*, 237.

Schultz, J., Lavielle, L., & Martin, C. (1987). The role of interface in carbon fiber-epoxy composites. *J. Adhesion*, *23*, 45.

Thielmann, F. (2004). Introduction into the characterization of porous materials by inverse GC. *J. Chrom. A*, *1037*, 115.

Thielmann, F. & Baumgartnen, E. (2000). Characterization of microporous aluminas by inverse GC. *J. Coll. Interf. Sci*., *229*, 418.

Thielmann, F., & Burnett, D. (2002). *Proceedings of AAPS, Toronto, Canada.* Arlington, VA: AAPS Press.

Thielmann, F., Naderi, M., Young, P., & Traini, D. (2006). Impact of lactose form on salbutamol sulphate lactose interactions in DPI formulations. *Proceedings of RDD* (p. 793; Boca Raton, Florida). Illinois: DHI.

Thielmann, F., & Pearse, D. (2002). Determination of surface heterogeneity profiles on graphite by finite concentration inverse gas chromatography. *J. Chrom. A, 969*, 323.

Ticehurst, M, York, P., Rowe, R., & Dwivedi. S. (1996). Characterization of the surface properties of a lactose monohydrate with inverse GC, used to detect batch variations. *Int. J. Pharm., 141*, 93.

van den Berg, C. & Bruin, S. (1981). *Water activity and its estimation in food systems.* San Diego, CA: Academic Press.

van Oss, C., & Good, R. (1989). Surface tension and solubility of polymers and biopolymers: the role of polar and apolar interfacial free energies. *J. Macromol. Sci.—Chem. A, 26*, 1183.

York, P., Ticehurst, M., & Osborn, J. (1998). Characterization of the surface energetics of milled DL propanolol hydrochloride using inverse GC and molecular modelling. *Int. J. Pharm., 174*, 179.

Young, P., & Price, R. (2006). Controlling and measuring active sites on carrier particles, *Proceedings of RDD*, p. 327; Boca Raton, FL.

Zeng, X., Martin, G., & Marriott, C. (2001). *Particulate interactions in dry powder formulations for inhalation*. London: Taylor & Francis.